PROTEINS: Structure, Function, and Genetics 21:214–225 (1995)

Modeling the Quinone-B Binding Site of the Photosystem-II Reaction Center Using Notions of Complementarity and Contact-Surface Between Atoms

Vladimir Sobolev and Marvin Edelman
Department of Plant Genetics, Weizmann Institute of Science, Rehovot 76100, Israel

ABSTRACT **Functional identity and significant similarities in cofactors and sequence exist between the L and M reaction center proteins of the photosynthetic bacteria and the D1 and D2 photosystem-II reaction center proteins of cyanobacteria, algae, and plants. A model of the quinone (Q_B) binding site of the D1 protein is presented based upon the resolved structure of the Q_B binding pocket of the L subunit, and introducing novel quantitative notions of complementarity and contact surface between atoms. This model, built without using traditional methods of molecular mechanics and restricted to residues in direct contact with Q_B, accounts for the experimentally derived functional state of mutants of the D1 protein in the region of Q_B. It predicts the binding of both the classical and phenol-type PSII herbicides and rationalizes the relative levels of tolerance of mutant phenotypes.** © 1995 Wiley-Liss, Inc.

Key words: photosynthetic reaction center, quinone binding site, D1 protein, herbicides

INTRODUCTION

Crystallization of the photosynthetic reaction center (PRC) from *Rhodopseudomonas viridis* and *Rhodobacter sphaeroides* led to a detailed structural picture of the anoxygenic bacterial reaction center and a vastly improved functional model of electron transfer involving pheophytin, chlorophylls, quinones, and iron cofactors.[1–3] The L and M subunits were found to participate symmetrically in the binding of the electron donor (special-pair chlorophylls) and the electron acceptor (quinone–iron complex),[4] with the quinone (Q_B) site on the L subunit accessible to a variety of electron-transfer-blocking substances which can displace Q_B from its binding site.[5]

Interestingly, the identical grouping of inhibitors also disrupted electron transfer in the photosystem II reaction center (RCII) of oxygenic phototrophs, i.e., plants, algae, and cyanobacteria.[6] One of these, the herbicide azidoatrazine, was shown to photoaffinity label the D1 protein of photosystem II[7] as well as the L subunit of the PRC.[8] Concomitantly, significant sequence homologies were recognized among the D1 and D2 proteins of plants and the L and M subunits of the photosynthetic bacteria, particularly in *Rhodobacter capsulatus*.[9] Based on these observations, the D1 and D2 proteins were proposed to correspond to L and M and form the reaction center core of photosystem II.[6,9,10] This hypothesis was soon verified experimentally by the isolation of a membrane complex from spinach consisting of the D1, D2, and cyt *b*559 proteins, pheophytin, chlorophyll, quinone, and iron, and capable of light-driven electron transport.[11] At the same time, the $Q_B^-Fe^{2+}$ signal in PRC and RCII were shown to be remarkably similar in their relationship to iron.[12]

The functional identity between the L subunit and the D1 protein spawned several structural models for D1 featuring transmembrane helical regions and cofactors bound at positions analogous to those found in the L subunit.[13–18] The general validity of the structural analogy at the experimental level derives from region-specific D1 antibodies which established the existence of five transmembrane helices and the antipodal positions of specific loop regions,[19] the parallel behavior of paired, site-directed mutants of the L and D1 proteins,[20–22] and parallel effects in D1 and L protein mutants following application of Q_B binding site inhibitors.[5,20,21,23]

Methods of molecular mechanics (see refs. 24 and 25) are traditionally used for prediction of protein chain structure and for fitting ligands in a binding site. These methods invariably include calculation of energy interaction between atoms, but there are two difficulties: (1) appropriate parameters have not been determined for all type of atoms, and (2) calculations were performed for structures in polar or nonpolar environment; however, for the D1 protein it is difficult to define in which type of environment the Q_B binding site is exposed.

Abbreviations: PRC, photosynthetic reaction center; RCII, reaction center of photosystem II; CF, complementarity function.

Received August 4, 1994; revision accepted November 1, 1994.

Address reprint requests to Vladimir Sobolev, Department of Plant Genetics, The Weizmann Institute of Science, Rehovot 76100, Israel.

In this paper we develop an approach which is not based on calculation of interaction energy, but rather, on analysis of contact between a cofactor and its binding site. A novel quantitative notion of contact surface between atoms is introduced and used to develop a model of the Q_B binding site of RCII in which a minimal set of amino acid residues forming the Q_B pocket is identified. This minimization further distinguishes our approach from those taken by others[14–18] describing the structure of the quinone binding region. Our approach can account for experimentally determined effects[26] of phenylurea, triazine, and phenol-type herbicides, and rationalizes the relative levels of tolerance for mutant phenotypes.

MATERIALS AND METHODS

All calculations were performed using a Personal Iris workstation (Silicon Graphics). Macromodel software[27] was used to visualize the structures obtained. The atomic coordinates (2.3 Å resolution) of the photosynthetic reaction center of *Rhodopseudomonas viridis,* deposited by Deisenhofer et al. in 1988–1989 (code name 1PRC) in the Brookhaven Protein Data Bank, Brookhaven National Laboratory,[28] were utilized throughout for building the model.

RESULTS AND DISCUSSION

Contact Surface Between Atoms

Lee and Richards[29] introduced the notion of the accessible surface of an atom as "the area on the surface of a sphere of radius R, on each point of which the center of a solvent molecule can be placed in contact with this atom without penetrating any other atom of the molecule." R is the sum of the van der Waals radii of atom A and the solvent molecule; viz.,

$$R = R_A + R_W.$$

To calculate the accessible surface of atom A, a computer program divides the surface of this imaginary sphere (sphere A) into small areas, calculates the distances (d_B) between the center of each small area and other atoms (B), and sums the squares of all small areas for which

$$d_B \geq R_B + R_W$$

where R_B is the van der Waals radius of any atom B. In our study, we define the contact surface of atom A with atom B (i.e., contact surface between atoms) as the area of the surface of sphere A on each point of which a solvent molecule, were it to be so placed, would penetrate atom B (Fig. 1). If the solvent molecule at some point of the sphere would penetrate several atoms, we postulate that this point is in contact surface only with the nearest of them. Clearly, the contact surface of atom A with atom B depends not only on the distance between their centers but also on the arrangement of the nearest atoms (Fig. 2).

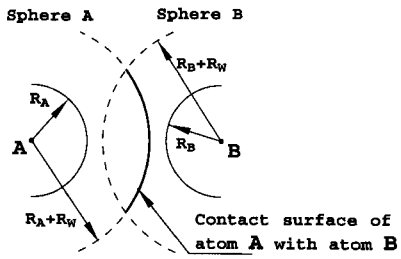

Fig. 1. Contact surface area of atom A with atom B. R_A and R_B represent van der Waals' radii of atoms A and B, respectively. R_W is the van der Waals' radius of the solvent molecule. Sphere A and sphere B extend to R_A+R_W and R_B+R_W, respectively.

Calculations of the accessible surface and contact surface of contacts for C, N, O, and S atoms were made using the atomic radii given by Lee and Richards,[29] and for other atoms, given by Bondi.[30] The radius of a solvent molecule was set equal to 1.4 Å.

Complementarity Function

An effective cofactor binding site should have an appropriate molecular structure which forms a large, attractive contact surface with its cofactor. We assume that the structural relationship between cofactor and binding site is given by

$$F_k = S_l - S_i \tag{1}$$

where S_l and S_i are sums of "legitimate" and "illegitimate" contact surfaces between cofactor atoms and binding site atoms. To aid us in defining the notions of "legitimate" and "illegitimate" contacts, we classify atoms as hydrophilic (oxygen and nitrogen), neutral (sulfur, and carbon atoms which have covalent bonds to hydrophilic atoms), or hydrophobic (other atoms). "Illegitimate" contact is defined as contact between hydrophobic and hydrophilic atoms, while all other contacts are considered "legitimate." We use function (1) as a measure of complementarity between any two molecular structures. This definition of complementarity is termed "complementarity function" (CF). Similar approaches, describing protein–protein complexes, have recently been reviewed by Cherfils and Janin.[31]

When looking for maximum complementarity as a function of atomic coordinates, unrealistically short distances between atoms can be avoided by introducing a "wall" function, such that expression (1) becomes

$$F_k = S_l - S_i - E_W \tag{2}$$

where

$$E_W = \sum_{ab} E_{ab}^W \tag{3}$$

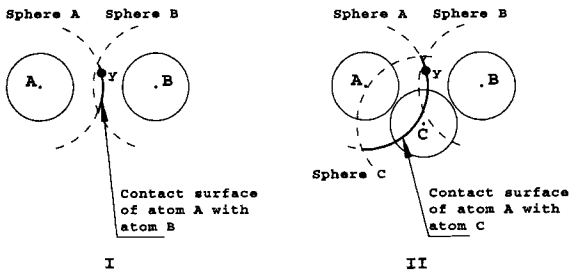

Fig. 2. Contact surface area of atom *A* with several atoms. If a solvent molecule at point Y of sphere A is so situated as to penetrate several atoms, we postulate that this point will be in contact surface only with the atom which is nearest to atom *A*. Therefore, in spite of the fact that the distance between atoms *A* and *B* in examples I and II is the same, in I, point Y will be in contact surface with atom *B*, while in II, it will be in contact surface with atom *C*.

and E_{ab}^{W} is 0 if the distance between atoms a and b is larger than the sum of van der Waals radii R_a and R_b, and infinite if the distance is smaller. Summation in (3) is executed for all atoms.

The use of infinite functions in optimization procedures, however, is inconvenient. Therefore, we have replaced E_{ab}^{W} with a function

$$E_{ab}^{W} = \begin{cases} 0 & \text{if } R_{ab} \geq R_0 \\ K(R_0 - R_{ab})^n, & \text{if } R_{ab} < R_0 \end{cases} \quad (4)$$

which is 0 if the distance between atoms is larger than some distance R_0, but rises very steeply as the distance becomes shorter. According to the atom–atom potential function theory,[32] repulsion between atoms takes place at distances shorter than the sum of their van der Waals radii. Based on this, we have chosen the values $R_0 = 0.9(R_a + R_b)$, $n = 12$ and $K = 10^6$ Å^{-10}. These values ensure that the term E_{ab}^{W} will be sharply dependent on interatomic distances but only a minor factor in structures with high complementarity.

We assume that a complex of any two molecules will have a structure with maximal CF. Therefore, to define the structure of a complex formed by a binding site and a ligand, we seek a maximum for F_k (2) as a function of six ligand coordinates and initiate the procedure of maximization from 1000 random points. These points are chosen to be within a box whose dimensions are 5 Å in all directions and located in a binding site. No space restriction exists, however, while searching for complementarity maxima. In the maximization procedure, we used the flexible polyhedron search method.[33] Summation in (3) is executed over all atoms of the ligand (a) and of the binding site (b).

The complementarity function proposed here may be generally useful for estimations of preferred structures, even when it is difficult to employ traditional methods of molecular docking (these methods have recently been reviewed by Kuntz et al.[34]). Such difficulties arise in cases where a molecule includes atoms for which relevant parameters have not yet been determined. They also arise in the case of a heterogeneous medium: at the boundary of a membrane phase and/or when it is impossible to estimate interactions with the nearest biomolecular structures. It should be pointed out that we define here only two types of contacts ("legitimate" and "illegitimate") for three types of atoms (hydrophilic, neutral, and hydrophobic). One can, however, generalize: For example, carbon atoms in the π-conjugated system can be considered neutral since the H-bond energy for these systems has been estimated and found to be significant.[24,35] Likewise, other types of contacts (for example, between charged groups) can be considered, and CF then defined as a sum of various contact surfaces with various weights.

Analysis of the Q_B Binding Niche in the Bacterial Photosynthetic Reaction Center

Calculation of the accessible surface of ubiquinone-1 (aside from the last two atoms of the tail) in the crystal structure of the bacterial PRC yields a value practically equal to 0 (Fig. 3). The ubiquinone binding site has the structure of a pocket with the quinone "head" (the entire molecule excluding the last three atoms of the tail) completely surrounded by a polypeptide chain composed solely of residues of the L protein (Table I). This conclusion follows from calculating the accessible and contact surfaces of the quinone in either the whole PRC or the ubiquinone binding domain (L protein from residue 184 to 232) alone, the values being identical. Furthermore, our calculations of contact surface of quinones in the bacterial PRC of *Rhodopseudomonas viridis* show that Q_A and Q_B binding sites are formed by residues of the M and L protein, respectively. We have reached the same conclusion by calculating the quinone contact surfaces in the PRC of *Rhodobacter sphaeroides* (atomic coordinates courtesy of J. Norris and M. Schiffer, Argonne National Laboratory). In all cases, these residues belong to the *D*, *de*, and *E* helices and the small *de*–*E* loop. Amino acid residues described by El-Kabbani et al.[36] as surrounding the quinones also belong exclusively to these regions.

We determined the structure which produces maximum complementarity between ubiquinone and the L protein chain from residue 184 to 232. In this structure ubiquinone is in a position similar to that in the PRC crystal, and has a maximum F_k of 316 Å^2. We repeated our search for maximum complementarity, but this time between ubiquinone and the model structure composed exclusively of residues calculated to be in contact with the quinone head (residues are listed in Table I). The structure was identical and the F_k value was exactly the same (316 Å^2). Local maxima for other structures were <160 Å^2. Such values can be expected for ubiqui-

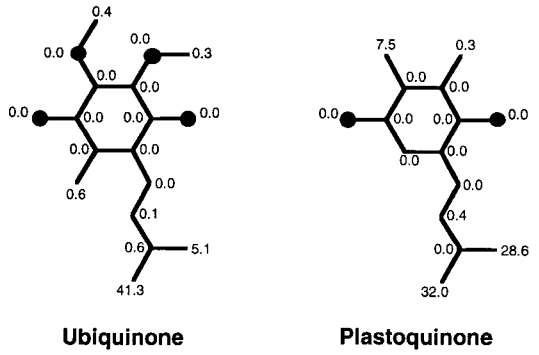

Fig. 3. Calculated accessible surfaces of ubiquinone atoms in the L subunit of the crystallized bacterial PRC, and plastoquinone atoms in the model Q_B binding pocket of the D1 protein. Oxygen atoms are marked by filled circles.

none complexed with any protein surface and do not signify specificity. In these cases the quinone head is not in the pocket but, rather, in partial contact with the protein chain.

On the basis of the above, we defined the minimal set of amino acid residues required for modeling the Q_B binding pocket in the L protein (Table I). A comparison of positions of ubiquinone in the crystal structure and calculated by maximization of complementarity is presented in Figure 4.

The Q_B Binding Niche in the D1 Protein

The arrangement of *trans*-membrane α-helices in the L and D1 proteins has been postulated to be very similar,[6,10] and boundaries of the D1 protein α-helices in the region of Q_B have been suggested.[4,6,13] In analogy to the PRC, we assume that the plastoquinone binding pocket in the RCII of plants is composed exclusively of D1 protein residues corresponding to those in the Q_B pocket of the L protein and in a similar position relative to the quinone coordinates. On this premise, His-215 and Leu-218 of the D1 protein are at the same position as His-190 and Leu-193 of the L protein, while the backbones of residues Phe-211, Met-214, Val-219, Ser-268, and Leu-271 of the D1 protein occupy the same positions as those of Ala-186, Leu-189, Ile-194, Ala-226, and Ile-229 of the L protein, respectively. In order to find the coordinates of these five residues in the D1 protein, we used the coordinates of the corresponding residues of the L protein and the replacement procedure of Macromodel software.[27] The structure obtained has an identical backbone conformation with no strong overlapping of side chain atoms. Only one of these replacements is unsatisfactory from the point of view of hydrophobicity: replacement of Ala-226 of the L protein by Ser-268 of D1. However, since in the L protein, quinone is in contact with Ala-226 only through the backbone atoms, replacement of Ala by Ser has no direct influence on the interaction of this residue with quinone.

Following Trebst[6,13] and Michel and Deisenhofer,[4] we assume that the role and position of Phe-255 in the *de*-helix of the D1 protein is the same as that of Phe-216 in the *de*-helix of the L protein; furthermore, that residues Ala-251 and His-252 of the D1 protein are also located in this helix and occupy the same positions as Glu-212 and Asn-213 of the L protein.[13,15] Glu-212 and Asn-213 are in contact with methoxy groups of ubiquinone.[37] Since plastoquinone lacks methoxy groups, replacement of these residues by more hydrophobic ones in D1 is not surprising.

In the L protein, ubiquinone is in contact with the hydroxyl group of Ser-223 and with the backbone atoms of Ile-224 and Gly-225. The composition and structure of the corresponding hydrophilic part of the Q_B pocket in the D1 protein are not readily determined from our assumptions. According to Ruffle et al.,[17] Ile-259, Tyr-263, and Ser-264 form this part of the pocket, while Tietjen et al.[15,38] have plastoquinone H-bonded with the hydroxyl of Ser-264 and amide NH of Phe-265. Energy calculations of complex formation between bacterial PRC and quinone have shown that H-bonds can form in this region either with Ser-223 and Gly-225 or with Ile-224 and Gly-225 (unpublished results in Egner et al.[18]). We restrict ourselves to replacement of Ser-223, Ile-224, and Gly-225 in the L protein by Ser-264, Phe-265, and Asn-266 of the D1 protein, respectively, but do not determine exactly which residue(s) of this hydrophilic region are in contact with plastoquinone. We are able to consider the contacts and interactions of herbicides with this part of the structure but do not discuss the functioning of the D1 protein modified by mutations in the region from residue 259 to 267.

The maximum complementarity of plastoquinone to our Q_B pocket structure of the D1 protein is 230 $Å^2$, while that for random conformation is about 140 $Å^2$. The maximum CF corresponds to a plastoquinone position (cf. Fig. 5a) very similar to that of ubiquinone in L protein. In this position, the accessible surface approaches zero for the atoms of the plastoquinone head (Fig. 3).

Properties of the D1 Mutants

It is commonly assumed that a major functional role of the loop between the *D* and *E* helices of the D1 protein is to bind quinone. Therefore, when a mutation disturbs the binding of Q_B, the function of RCII is likely to be disturbed as well. Our model of the Q_B pocket consists of residues of the *D*, *de*, and *E* helices, and the short *de*–*E* loop. This structure is fairly rigid and the influence of substitutions, deletions, or additions will depend mainly on the resulting changes in interactions between side chain and quinone (see, e.g., Chirino et al.[39]). Such interactions, in turn, will significantly depend on the hydrophobicity and bulkiness of residues.

TABLE I. Contact Surfaces (Å^2) of Ubiquinone (UQ), Plastoquinone (PQ), and Herbicides in the Q_B Pockets

L protein		D1 protein					
				Herbicides			
UQ	Contact residues	Contact residues	PQ	Diuron	Atrazine	BNT	Ioxynil
0.6	A186	F211	0.1	11.6	14.1	0.4	4.8
22.8	L189	M214	5.0	53.2	16.8	19.3	26.3
60.5	H190	H215	65.8	30.7	30.9	93.4	46.1
12.4	L193	L218	23.4	17.4	13.0	59.9	51.4
9.6	I194	V219	7.6	6.0	0.0	39.4	39.8
48.1	E212	A251	8.1	18.5	45.3	20.6	10.9
21.6	N213	H252	13.5	28.6	36.8	9.3	45.9
44.5	F216	F255	46.8	50.4	42.7	21.7	32.6
27.0	S223						
3.1	I224	*de–E* loop	78.4	48.3	84.1	77.3	48.4
34.2	G225	(259–267)					
42.2	A226	S268	20.1	49.7	16.7	27.5	9.7
17.6	I229	L271	31.5	44.8	62.0	33.9	50.5

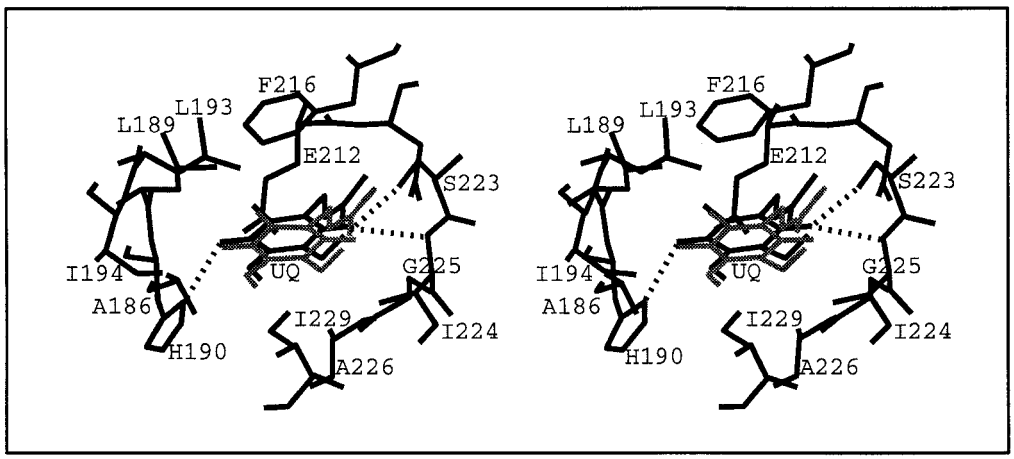

Fig. 4. Stereo view of the ubiquinone molecule in the Q_B binding pocket of the L protein. Gray, position in crystal structure. Black, position corresponding to maximum complementarity in our model of the Q_B binding pocket.

In our model, residues of the *D–de* loop from Thr-220 to Asn-247 do not participate significantly in the plastoquinone binding pocket. We predict that modification of this region will not have a direct influence on quinone binding. Indeed, analyses of growth rates and oxygen evolution for 15 mutants in the region from Thr-220 to Asn-247 indicate only a weak influence on protein function.[22] In line with this, phylogenetic variation for 41 sequences of the D1 protein (Svensson et al.[38] and J. Hirschberg, personal communication) is considerably greater in the *D–de* loop region than in the adjacent helical and *de–E* loop regions (cf. Kless et al.[22]).

Reported D1 protein mutations directly relevant to our model are listed in Table II. We predict that in mutant ΔAA250-1, + Y246-7 the insertion of Tyr between residues 246 and 247 has little influence on quinone binding, but deletion of the alanine residues removes Ala-251 from contact with plastoquinone. Therefore, the overall influence of this mutation on Q_B function should be very strong, as indeed found (cf. Table II). The slight amount of RCII function retained by this mutant may be due to inclusion of Val-249 in the *de*-helix of the mutant.

Mutation AH251-2VP involves two residues with direct contacts to quinone. We therefore expect the influence of this mutation on RCII function to be catastrophic. In addition, drastic effects may be due to significant structural perturbation caused by introduction of Pro in the helix. This agrees with the data of Table II. We note however that in the L protein, Glu-212 and Asp-213, which are analogous to Ala-251 and His-252 of the D1 protein, take part in the process of quinone protonation.[41–45] In the D1 protein, His-252 may be involved in similar chains of protonatable residues.[15,46] Thus, we cannot ex-

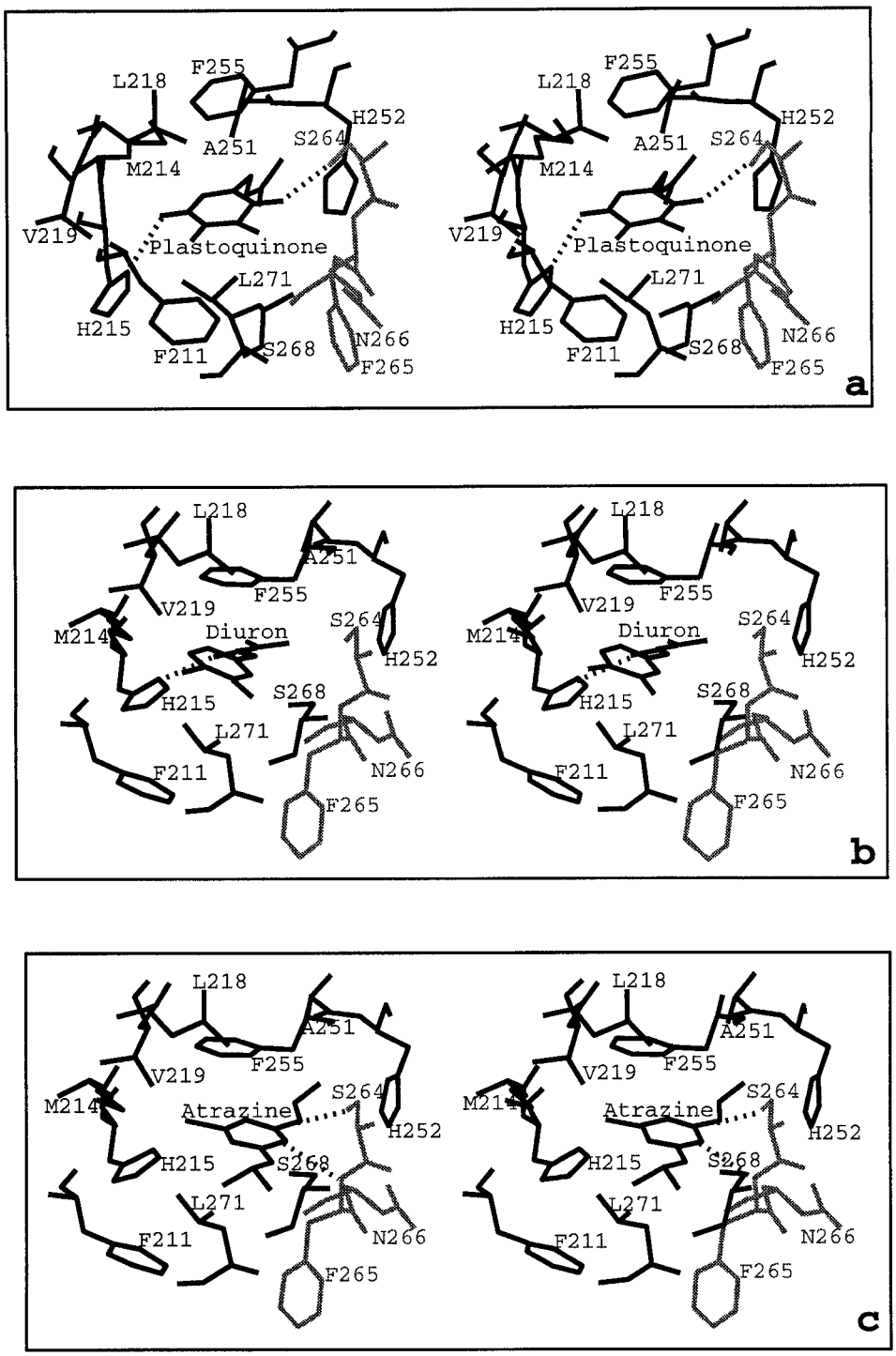

Fig. 5a–c.

clude that destruction of protein function in mutant AH251-2VP derives from disruption of proton transfer rather than, or in addition to, disruption of Q_B binding.

Tyr-254 is not a residue predicted by us to be in contact with the quinone. However, the side chain of the corresponding residue in the L protein (Tyr-215) has large contact with the ring of Phe-216 (28 Å^2). An analogous contact of Tyr-254 with the ring of Phe-255 in the D1 protein is expected to be important for formation of the hydrophobic core in this region of RCII. Our model correctly predicts that

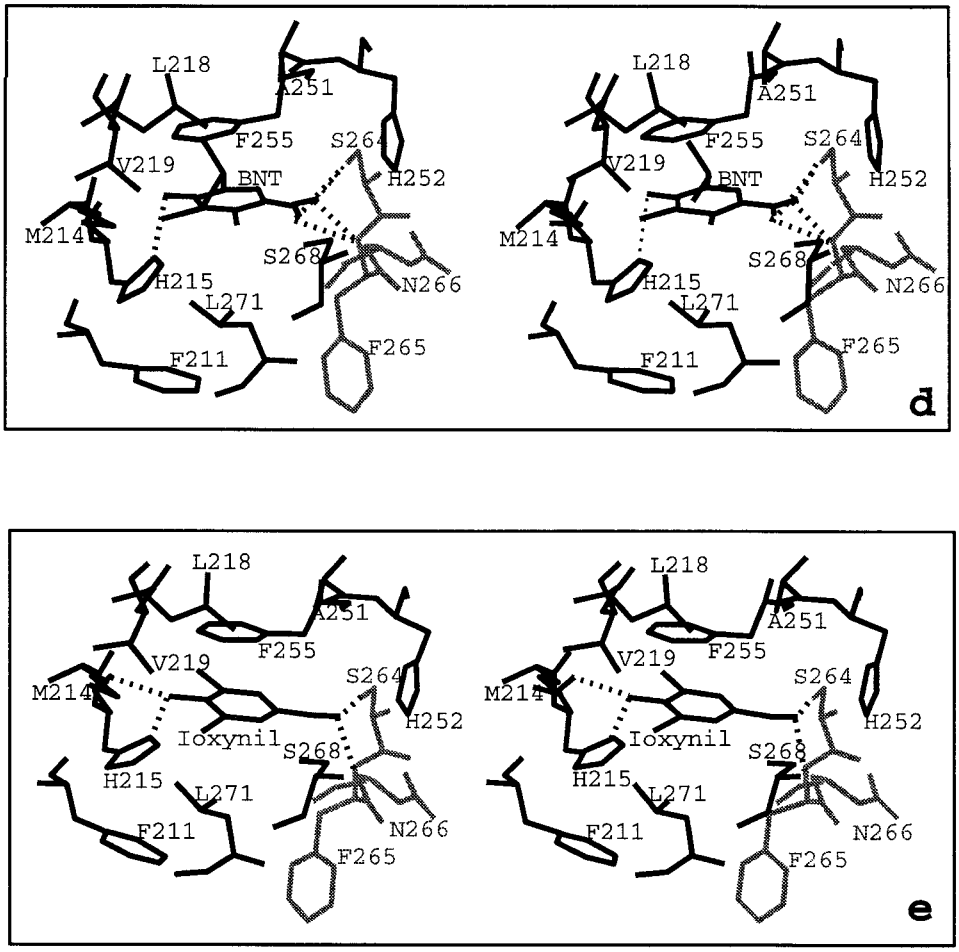

5

Fig. 5. Stereo view of plastoquinone and herbicide molecules in the Q_B binding pocket of the D1 protein: (**a**) plastoquinone, (**b**) diuron, (**c**) atrazine, (**d**) bromonitrothymol (BNT), (**e**) ioxynil. All of the structures have been assessed for chemical acceptability.

substitution of Tyr-254 with hydrophobic phenylalanine does not markedly influence RCII activity, while substitution with hydrophilic threonine or serine considerably suppresses function (Table II).

Residue Phe-255 forms an important part of the quinone binding pocket. Thus, the fatal consequences of its deletion, as in mutation ΔYFGR254-7 (which probably also destroys the *de*-helix), or of its being sterically hindered as in mutation F255W (where bulkier Trp replaces Phe), can readily be understood (Table II). We cannot, however, exclude another possible influence of E255W mutation. Phe-255 has a large hydrophobic contact with plastoquinone and this contact should give essential contribution in binding energy. Maybe Trp, with its larger ring, stabilizes the complex with quinol. After the quinone accepts two electrons and is protonated, the binding pocket cannot eject the quinol, which inhibits further process. On the other hand, our model leads us to predict that mutants F255Y, F255Y+S264A, or F255L+S264A will bind plastoquinone. This is because Tyr has practically the same hydrophobic ring as Phe (the affinity of F255Y to some quinone-replacing inhibitors may even increase because of additional H-bonding[47,48]), while Leu is both hydrophobic and not bulkier than Phe). The normal growth of mutant F255L+S264A (Table II) suggests that interaction of the aromatic ring of Phe-255 may not be critical for Q_B binding. Concerning the affect of mutation S264A in the double mutants discussed above, we note that Horovitz et al.[49] have shown a lack of interaction between Ph-255 and Ser-264. Most experimental data[21,22] suggest that replacement of Ser-264 in the D1 protein does not directly influence Q_B function. We emphasize, however, that we cannot discuss mutation of Ser-264 based on our model.

Arg-257 is thought to be in the *de*-helix facing away from the quinone niche. We therefore expect that this residue is not in contact with quinone. However, replacement of charged Arg by hydrophobic Val (Table II) may cause global changes in the

TABLE II. Photoautotrophic Growth Rate for *Synechocystis* Mutants Altered in the Q_B Binding Pocket of the D1 Protein

Mutant strain	Growth rate	Reference*
ΔAA250-1, + Y246-7	+	a
AH251-2VP	−	a
Y254F	+ + +	b
Y254T	+	a
Y254S	−	b
ΔYFGR254-7	−	a
F255Y	+ + +	c
F255W	−	b
F255Y + S264A	+ + +	c
F255L + S264A	+ + +	c
R257V	+ +	a
L258F + Y237F	−	a
L258I + Y237F	+ + +	a
S264A	+ +	c
L271V	+ + +	b
L271M	+ +	b
L271A	+	b
L271S	−	b

*(a) Data for *Synechocystis* PCC 6803 from Kless et al.[22] (b) Data for *Synechocystis* PCC 6803 from Ohad and Hirschberg.[21] (c) Data for *Synechocystis* PCC 7942 from Ohad and Hirschberg.[21]

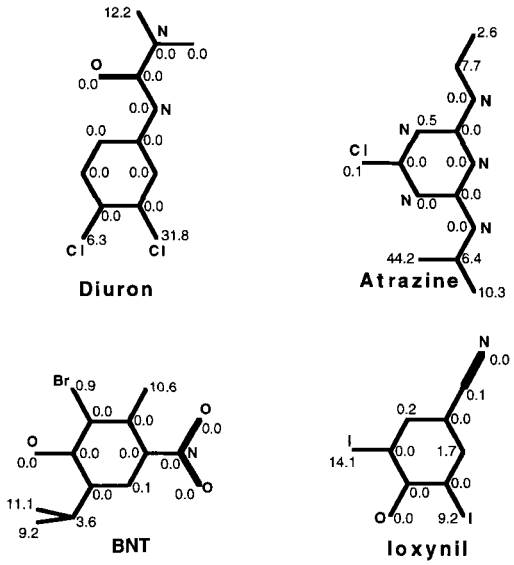

Fig. 6. Chemical structure of herbicides fitted into the modeled Q_B binding pocket of the D1 protein. Numbers represents atomic accessible surfaces in the herbicide–pocket complex.

position of the *de*-helix, effects of which we are unable to predict by our approach.

Our model does not include Leu-258 in the Q_B binding pocket, and its substitution by Ile is not predicted to, nor does it cause, severe changes in function (Table II). However, Leu-258 is apparently in close proximity to Phe-255 in the *de*-helix.[13] Thus, the fatal effect of mutation L258F (Table II) may be due to steric restrictions, the volume of the Phe side chain being larger than that of Leu. Concerning Tyr-237 in the double mutations, our model does not predict any direct influence on quinone binding for this residue in agreement with experimental data for the mutation Y237F.[22]

Residue Leu-271 has large hydrophobic contact with plastoquinone (cf. Table I); therefore, we can predict that the consequences of its substitution will depend on hydrophobicity. Influence of hydrophobicity and bulkiness at position 271 of the D1 protein, and in the corresponding position, 229, of the L protein, has been discussed by Ohad and Hirschberg[21] and Bylina and Youvan,[50] respectively. Indeed, replacement of Leu-271 by Val does not affect growth rate while mutation L271S is fatal (Table II).

Herbicide Binding

Several herbicides which affect PS II compete with plastoquinone and replace it from its binding pocket.[51] Representative PS II herbicides of different chemical classes which have been fitted into the modeled pocket are shown in Figure 6. The maximum complementarity to the Q_B binding pocket was found for each herbicide (Table III) and the structures obtained are presented in Figure 5b–e. The main term in the complementarity function (2) is the surface of "legitimate" contact (S_l). The other terms (S_i and E_W) play an essential role in the relative value of CF for different compounds. The low values of accessible surface of most atoms (Fig. 6) stress the high complementarity of the herbidides to the Q_B binding pocket. The CF values for herbicides in the pocket are larger than that of the native substrate, plastoquinone (Table III). This explains their effectiveness as photosynthesis inhibitors. We have also calculated the contact surface of herbicides with residues of the quinone binding pocket (Table I).

In our model, formation of H-bonds between N atoms of atrazine and the hydrophilic region composed of residues of the *de–E* loop is highly probable (Fig. 5c). Similar structures have been obtained in theoretical studies.[15,18] The next most likely structure has considerably lower complementarity (by 29 Å^2). As opposed to atrazine, formation of a H-bond between the oxygen atom of diuron and His-215 (Fig. 5b) is more probable than between either the oxygen atom or NH group of diuron and the hydrophilic region of the *de–E* loop, but differences in complementarity are only 5 and 9 Å^2, respectively. Nevertheless, the likelihood of the structure in Figure 5b receives support from theoretical calculations[18,52] and EPR data.[53] This structure is also supported by Sinning[5] based on X-ray crystallographic analysis of PRC bound diuron.

The binding site of phenol type herbicides in the D1 protein is still under discussion.[54–56] Our calculations predict replacement of plastoquinone by BNT or ioxynil in the binding pocket (Table III).

TABLE III. Complementarity Maxima (Å²) for Plastoquinone and Herbicides in the Q_B Binding Pocket of the D1 Protein

	Complementarity function*			
Molecule	F_k	S_l	S_i	E_W
Plastoquinone	230	282	18	34
Diuron	320	345	14	11
Atrazine	281	331	31	19
BNT	269	365	37	60
Ioxynil	273	346	20	52

*Terms are given in Eq. (2).

These herbicides, like plastoquinone (Fig. 5a), form hydrogen bonds with both His-215 and the hydrophilic region of the *de–E* loop. In our model, hydrogen bonds are formed between the hydroxyl group of BNT and His-215, and the nitro group of BNT and the hydrophilic region of the *de–E* loop (Fig. 5d). Although the next best structure (with hydrogen bonds formed between the hydroxyl group of BNT and hydrophilic region of the *de–E* loop and the nitro group of BNT and His-215) has practically the same complementarity function, experimental data[57] (see below: *Stronger steric effects*) favor the model presented in Figure 5d. The third most likely structure has considerably lower complementarity (by 24 Å²).

Ioxynil is also bound by the two hydrophilic regions of the Q_B pocket in a similar way. There is close contact between the hydroxyl group of ioxynil and the imidazole NH group of His-215 on the one hand, and the cyan group of this herbicide and the *de–E* loop on the other (Fig. 5e). This orientation is supported by the binding of 2-azido ioxynil to Val-249[58]; in our structure, the carbon atom in position 2 of the ioxynil ring has contact surface of ~5 Å² with the nearby residue, Ala-251. The next most likely structure exhibits the same hydrogen bonds but with a complementarity lower by 5 Å².

The effect of a herbicide is commonly described by the molar concentration of inhibitor reducing electron transfer by 50% (I_{50}). Herbicide resistance in D1 protein mutants is caused by changes in herbicide binding as well as quinone affinity,[59] the relative values being unclear. Therefore, discussion of changes of <10-fold in herbicide resistance is of questionable value at this stage.

A compilation of the effects of herbicides (I_{50}) on D1 mutants altered in one or more of the residues forming or contacting the modeled quinone pocket is shown in Table IV. We assume that differences in herbicide binding caused by D1 protein mutations can be explained by changes in: steric contacts (especially if these changes perturb specific interactions), interactions of various polar and nonpolar parts of the herbicide with the point of mutation, and structural rearrangements in the binding pocket. The last two factors often result in lethality

TABLE IV. Relative Photosystem II Activity (I_{50} Mutant/I_{50} Wild Type) of D1 Protein Mutants Altered in Residues in Contact with Plastoquinone or in Surrounding α-Helices

Mutant	Diuron	Atrazine	BNT	Ioxynil
F211S	$1^{60},2^{61}$	$7^{61},10^{60}$	—	3^{62}
V219I	$7–32^{47,63}$	$2–4^{61,63}$	2^{47}	$7^{63},50^{47}$
SS221-2LA	560^{22}	24^{22}	2^{22}	6^{22}
A251V	$5^{55,65},8^{47}$	$25^{47,65,66}$	8^{47}	$25^{62},40^{47}$
Y254F	1^{21}	1^{21}	—	—
F255Y	$0.6–1.5^{21,47,64}$	$15–25^{22,47,64}$	0.6^{47}	2.5^{47}
G256D	$3^{67},10^{47}$	$15^{67},84^{47}$	—	—
R257V	38^{22}	30^{22}	0.3^{22}	0.8^{22}
L271V	3^{21}	2^{21}	—	—
L271M	1^{21}	3^{21}	—	—
L271A	1^{21}	2^{21}	—	—
L275F	1^{67}	3^{67}	—	—
L275P	1^{61}	5^{61}	1.6^{47}	0.2^{47}

or severe changes in growth rate (cf., Table II). We are unable to predict the affects of herbicides on such mutants (e.g., G256D or R257V in Table IV) by our approach. We therefore limit our discussion to steric contacts.

Weak steric effects: Plastoquinone as well as the herbicides under discussion have relatively minor contact surfaces with Phe-211 (Table I). Therefore, substitution of this residue by one not bulkier, as in mutant F211S, should not lead to substantial changes in binding pocket affinities. We predict only minor changes in herbicides resistance and the data in Table IV bear out our prediction.

Plastoquinone as well as the herbicides analyzed have large contact surfaces with Phe-255 (Table I). However, as discussed above, the substitution of Phe-255 by Tyr does not change pocket affinity to the ligands; consequently, a change in I_{50} values versus wild type is not expected. This is in a good agreement with the experimental date for diuron, BNT, and ioxynil (Table IV). As already emphasized by Egner et al.,[18] the situation for atrazine is not readily explained. Quantum chemical calculations of interaction of the quinine and atrazine rings with those of Phe and Tyr may be of aid here. In our model, the distance between the ring centers of atrazine and Phe-255 is shorter by 0.5 Å than that between the ring centers of plastoquinone and Phe-255.

Similarly, according to our model, plastoquinone and herbicides both have large hydrophobic contact with L271. However, amino acid replacements L271V, L271M, and L271A cannot cause strong steric contacts since the Leu side chain is bulkier than any of the replacing residues. Therefore these substitutions can be expected to affect hydrophobic contacts of both plastoquinone and herbicides with residue 271 and do not disturb hydrophilic contacts, resulting in only small changes in resistance (Table IV).

Residues 254 and 275 are not in contact with any of the 4 herbicides being analyzed. Therefore, mutations Y254F, L275F, and L275P are not expected by us to lead to significant changes in herbicide binding, as indeed is the case (Table IV).

Stronger steric effects: There is only modest surface contact between diuron and Val-219 (Table I). However, replacement of the latter by bulkier Ile in mutant V219I may disturb the H-bond with His-215. As diuron is calculated in our model to form an H-bond only with His-215 (Fig. 5b), even mild perturbation of this bond can be expected to have a significant affect (Table IV). Atrazine, on the other hand, is not in contact with V219 (Table I, Fig. 5c). Thus, appreciable effects with this inhibitor at this position are not expected by us, and, indeed, were not found (Table IV). The phenol herbicide ioxynil has large surface contact with V219 (Table I). Thus, substitution of this residue by bulkier Ile can be expected to cause steric restrictions, lower affinity, and increase herbicide resistance. This prediction is borne out (Table IV). BNT also has large surface contact with Val-219 (Table I); however, resistance to BNT is not increased in the V219I mutant (Table IV). Analysis of atom–atom contributions shows that the isopropyl group at the R^6 position of the phenyl ring is the major contributor to BNT–Val-219 contact (Fig. 5d). As rotation of the isopropyl group can readily occur, energetically unfavorable steric hindrance with Ile can be avoided. However, our model predicts that such rotation will not suffice when bulkier groups are substituted at the R^6 position. This is in excellent agreement with the recent data of Jansen et al.[57] We calculated the bulkiness of the substituants at the R^6 position used by these authors (*tert*-butyl, cyclopentyl, phenyl, cyclohexyl, and benzyl). We find that the relative increases in I_{50} they obtained[57] (1, 13, 20, 40, 48) exhibit a strict linear dependence on bulkiness (77, 85, 92, 99, and 107 $Å^3$, respectively).

Serine residues 221 and 222 are thought to be part of the *D*-helix.[4,13] We suggest that the strong resistance to diuron in the SS221-2LA mutant (Table IV) is due to pocket deformation by Leu at position 221. The corresponding L protein residues, Ser-196 and Val-197, have contact surfaces (total of 47 $Å^2$) with Leu-193 and Ile-194, which form part of the ubiquinone pocket and correspond to D1 protein residues 218 and 219. We therefore expect that Leu-221 and Ala-222 in the mutated D1 protein will affect the positions of Leu-218 and Val-219 and may disturb the H-bond formed between diuron and His-215 (Fig. 5b). Atrazine does not form any H-bonds in this region (Fig. 5c), hence a much lower resistance to this herbicide (Table IV) is to be expected. BNT (Fig. 5d), ioxynil (Fig. 5e), and plastoquinone (Fig. 5a) all have contacts with residues 218 and 219, and H-bond with His-215, and H-bonds with the hydrophilic *de–E* loop region (Ser-264, Phe-265, and Asp-266). We therefore predict that similar changes in the binding of plastoquinone and herbicides occur resulting in small changes in resistance to BNT or ioxynil (Table IV).

In our model, all four herbicides under consideration have contact surfaces with Ala-251 larger than that of plastoquinone (Table I). Ajlani et al.[62] and Wildner et al.[47] have previously discussed the steric factors leading to the increased resistance of mutant A251V to herbicides.

ACKNOWLEDGMENTS

We thank Drs. J. Norris and M. Schiffer, Argonne National Laboratory, for providing the atomic coordinates of the PRC of *Rhodobacter sphaeroides*, and A. Girshovich, J. Gressel, A. Horovitz, and E. Yakobson for helpful discussions and comments on the manuscript. The research was supported in part by the Forschheimer and Wilstätter Centers at the Weizmann Institute of Science. This paper is dedicated to Prof. Achim Trebst on his sixty-fifth birthday.

REFERENCES

1. Deisenhofer, J., Michel, H. The photosynthetic reaction centre from the purple bacterium *Rhodopseudomonas viridis*. EMBO J. 8:2149–2170, 1989.
2. Feher, G., Allen, J.P., Okamura, M.Y., Rees, D.C. Structure and function of bacterial photosynthetic reaction centres. Nature (London) 339:111–116, 1989.
3. Chang, C.-H, El-Kabbani, O., Tiede, D., Norris, J., Schiffer, M. Structure of the membrane-bound protein photosynthetic reaction center from *Rhodobacter sphaeroides*. Biochemistry 30:5352–5360, 1991.
4. Michel, H., Deisenhofer, J. Relevance of the photosynthetic reaction center from purple bacteria to the structure of photosystem II. Biochemistry 27:1–7, 1988.
5. Sinning, I. Herbicide binding in the bacterial photosynthetic reaction center. Trends Biochem. Sci. 17:150–154, 1992.
6. Trebst, A. The topology of the plastoquinone and herbicide binding peptides of photosystem II in the thylakoid membrane. Z. Naturforsch 41c:240–245, 1986.
7. Pfister, K., Steinback, E., Gardner, G, Arntzen, J. Photoaffinity labeling of an herbicide receptor protein in chloroplast membranes. Proc. Natl. Acad. Sci. U.S.A. 78:981–985, 1981.
8. de Vitry, C., Diner, B.A. Photoaffinity labeling of the azidoatrazine receptor site in reaction centers of *Rhodopseudomonas sphaeroides*. FEBS Lett. 167:327–331, 1984.
9. Hearst, J.E. Primary structure and function of the reaction center polypeptides of *Rhodopseudomonas capsulata*—the structural and functional analogies with the photosystem II polypeptides of plants. In: "Photosynthesis III." Staehelin, L.A., Arntzen, C.J. (eds.). Berlin: Springer-Verlag, 1986: 382–389.
10. Deisenhofer, J., Epp, O., Miki, K., Huber, R., Michel, H. Structure of the protein subunits in the photosynthetic reaction centre of *Rhodopseudomonas viridis* at 3 Å resolution. Nature (London) 318:618–624, 1985.
11. Namba, O., Satoh, K. Isolation of a photosystem II reaction center consisting of D-1 and D-2 polypeptides and cytochrome b-559. Proc. Natl. Acad. Sci. U.S.A. 84:109–112, 1987.
12. Rutherford, A.W. How close is the analogy between the reaction centre of PSII and that of purple bacteria? 2. The electron acceptor side. In: "Progress in Photosynthesis Research," Vol. I. Biggins, J. (ed.) Dordrecht, The Netherlands: Martinus Nijhoff, 1987: 277–283.
13. Trebst, A. The three-dimensional structure of the herbi-

cide binding niche on the reaction center polypeptides of photosystem II. Z. Naturforsch 42c:742–750, 1987.
14. Bowyer, J., Hilton, M., Whitelegge, J., Jewess, P., Camilleri, P., Crofts, A., Robinson, H. Molecular modeling studies of the binding of phenylurea inhibitors to the D1 protein of photosystem II. Z. Naturforsch 45c:379–387, 1990.
15. Tietjen, K.G., Kluth, J.F., Andree, R., Haug, M., Lindig, M., Muller, K.H., Wroblowsky, H.J., Trebst, A. The herbicide binding niche of photosystem II-A model. Pestic. Sci. 31:65–72, 1991.
16. Ohad, N., Keasar, C., Hirschberg, J. Molecular modeling of the plastoquinone (Q_B) binding site in photosystem II. In: "Research in Photosynthesis," Vol. II. Murata, N. (ed.). The Netherlands: Kluwer Acad. Publ., 1992: 223–226.
17. Ruffle, S.V., Donnelly, D., Blundell, T.L., Nugent, J.H.A. A three dimensional model of the photosystem II reaction centre of *Pisum sativum*. Photosyn. Res. 34:287–300, 1992.
18. Egner, U., Hoyer, G.-A., Saenger, W. Modeling and energy minimization studies on the herbicide binding protein (D1) in photosystem II of plants. Biochim. Biophys. Acta 1142: 106–114, 1993.
19. Sayre, R.T., Anderson, B., Bogorad, L. The topology of a membrane protein: The orientation of the 32 kd Qb-binding chloroplast thylakoid membrane protein. Cell 47:601–608, 1986.
20. Bylina, E.J., Jovine, V.M., Youvan, D.C. A genetic system for rapidly assessing herbicides that complete for the quinone binding site of photosynthetic reaction centers. Biotechnology 7:69–74, 1989.
21. Ohad, N., Hirschberg, J. Mutations in the D1 subunits of photosystem II distinguish between quinone and herbicide binding sites. Plant Cell 4:273–282, 1992.
22. Kless, H., Oren-Shamir, M., Malkin, S., McIntosh, L., Edelman, M. The *D-E* region of the D1 protein in involved in multiple quinone and herbicide interactions in photosystem II. Biochemistry 33:10501–10507, 1994.
23. Sinning, I., Michel, H., Mathis, P., Rutherford, A.W. Characterization of four herbicide-resistant mutants of *Rhodopseudomonas viridis* by genetic analysis, electron paramagnetic resonance, and optical spectroscopy. Biochemistry 28:5544–5553, 1989.
24. Basharov, M.A., Vol'kenshtein, M.V., Golovanov, I.B., Nauchitel', V.V., Sobolev, V.M. The fragment-fragment interaction method. Part 1. Estimating molecule-molecule interactions. J. General Chem., U.S.S.R. 59:435–447, 1989.
25. Wade, R.C. Molecular interaction fields. In: "3D QSAR in Drug Design. Theory, Methods and Applications." Kubinyi, H. (ed.). Leiden: ESCOM, 1993: 486–505.
26. Jansen, M.A.K., Gaba, V., Greenberg, B.M., Mattoo, A.K., Edelman, M. UV-B driven degradation of the D1 reaction-center protein of photosystem II proceeds via plastosemiquinone. In: "Photosynthetic Responses to the Environment." Yamamoto, H.Y., Smith, C.M. (eds.). Rockville, MD: Plant Physiol. Soc. Publ., 1993: 142–149.
27. Mohamadi, F., Richards, N.G.J., Guida, W.C., Liskamp, R., Lipton, M., Caufield, C., Chang, G., Hendrickson, T., Still, W.C. Macromodel—An integrated software system for modeling organic and bioorganic molecules using molecular mechanics. J. Comp. Chem. 11:440–467, 1990.
28. Bernstein, F.C., Koetzle, T.F., Williams, G.J.B., Meyer, E.F., Rodgers, J.R., Kennand, O., Shimanouchi, T., Tasumi, M. The protein data bank: A computer based archival file for macromolecular structures. J. Mol. Biol. 112: 535–542, 1977.
29. Lee, B., Richards, F.M. The interpretation of protein structure: Estimation of static accessibility. J. Mol. Biol. 55: 379–400, 1971.
30. Bondi, A. Van der Waals volumes and radii. Phys. Chem. 68:441–451, 1964.
31. Cherfils, J., Janin, J. Protein docking algorithms: simulating molecular recognition. Curr. Opin. Struct. Biol. 3:265–269, 1993.
32. Kitaigorodskii, A. "Molecular Crystals and Molecules." New York: Academic Press, 1973.
33. Himmelblau, D.M. "Applied Nonlinear Programming." New York: McGraw-Hill, 1972.
34. Kuntz, I.D., Meng, E.C., Shoichet, B.K. Structure-based molecular design. Acc. Chem. Res. 27:117–123, 1994.
35. Levitt, M., Perutz, M.F. Aromatic rings act as hydrogen bond acceptors. J. Mol. Biol. 201:751–754, 1988.
36. El-Kabbani, O., Chang, C.-H., Tiede, D., Norris, J., Schiffer, M. Comparison of reaction centers from *Rhodobacter sphaeroides* and *Rhodopseudomonas viridis:* Overall architecture and protein-pigment interactions. Biochemistry 30:5361–5369, 1991.
37. Paddock, M.L., Rongey, S.H., Abresch, E.C., Feher, G., Okamura, M.Y. Reaction centers from three herbicide-resistant mutants of *Rhodobacter sphaeroides* 2.4.1: Sequence analysis and preliminary characterization. Photosyn. Res. 17:75–96, 1988.
38. Tietjen, K.G., Draber, W., Goossense, J., Jansen, J.R., Kluth, J.F., Schindler, M., Wroblowsky, H.-J., Hilp, U., Trebst, A. Binding of triazines and triazinones in the Q_B-binding niche of photosystem II. Z. Naturforsch 48c:205–212, 1993.
39. Chirino, A.J., Lous, E.J., Huber, M., Allen, J.P., Schenck, C.C., Paddock, M.L., Feher, G., Rees, D.C. Crystallographic analyses of site-directed mutants of the photosynthetic reaction center from *Rhodobacter sphaeroides*. Biochemistry 33:4584–4593, 1994.
40. Svensson, B., Vass, I.E., Styring, S. Sequence analysis of the D1 and D2 reaction center protein of photosystem II. Z. Naturforsch 46c:765–776, 1991.
41. Michel, H., Epp, O., Deisenhofer, J. Pigment-protein interactions in the photosynthetic reaction centre from *Rhodopseudomonas viridis*. EMBO J. 5:2445–2451, 1986.
42. Paddock, M.L., Rongey, S.H., Feher, G., Okamura, M.Y. Pathway of proton transfer in bacterial reaction centers: Replacement of glutamic acid 212 in the L subunit by glutamine inhibits quinone (secondary acceptor) turnover. Proc. Natl. Acad. Sci. U.S.A. 86:6602–6606, 1989.
43. McPherson, P.H., Schönfeld, M., Paddock, M.L., Okamura, M.Y., Feher, G. Protonation and free energy changes associated with formation of Q_BH_2 in native and Glu-L212→Gln mutant reaction centers from *Rhodobacter sphaeroides*. Biochemistry 33:1181–1193, 1994.
44. Takahashi, E., Wraight, C.A. A crucial role for Asp^{L213} in the proton transfer pathway to the secondary quinone of reaction centers from *Rhodobacter sphaeroides*. Biochim. Biophys. Acta 1020:107–111, 1990.
45. Paddock, M.L., Rongey, S.H., McPherson, P.H., Juth, A., Feher, G., Okamura, M.Y. Pathway of proton transfer in bacterial reaction centers: role of aspartate-L213 in proton transfers associated with reduction of quinone to dihydroquinone. Biochemistry 33:734–745, 1994.
46. Nixon, P.J., Chisholm, D.A., Diner, B.A. Isolation and functional analysis of random and site-directed mutants of photosystem II. In: "Plant Protein Engineering." Shewry, P.R., Gutteridge, S. (eds.). Cambridge: Cambridge University Press, 1992:93–141.
47. Wildner, G.F., Heisterkamp, U., Trebst, A. Herbicide cross-resistance and mutations of the *psb*A gene in *Chlamydomonas reinhardtii*. Z. Naturforsch 45c:1142–1150, 1990.
48. Oettmeier, W., Hilp, U., Draber, W., Fedtke, C., Schmidt, R.R. Structure-activity relationship of triazinone herbicides on resistant weeds and resistant *Chlamydomonas reinhardtii*. Pestic. Sci. 33:399–409, 1991.
49. Horovitz, A., Ohad, N., Hirschberg, J. Predicted effects on herbicide binding of amino acid substitutions in the D1 protein of photosystem II. FEBS Lett. 243:161–164, 1989.
50. Bylina, E.J., Youvan, D.C. Genetic engineering of herbicide resistance: Saturation mutagenesis of isoleucine 229 of the reaction center L subunit. Z. Naturforsch 42c:769–774, 1987.
51. Bowyer, J.R., Camilleri, P., Vermaas, W.F.J. Photosystem II and its interactions with herbicides. In "Herbicides." Baker, N.R., Percival, M.P. (eds.). Amsterdam: Elsevier, 1991: 27–85.
52. Mackay, S.P., O'Malley, P.J. Molecular modeling of the interaction between DCMU and the Q_B-binding site of photosystem II. Z. Naturforsch 48c:191–198, 1993.
53. Diner, B.A., Petrouleas, V. Q_{400}, the non-heme iron of the photosystem II iron quinone complex. A spectroscopic probe of quinone and inhibitor binding to the reaction center. Biochim. Biophys. Acta 895:107–125, 1987.
54. Creuzet, S., Ajlani, G., Vernotte, C., Astier, C. A new ioxynil-resistant mutant in *Synechocystis* PCC 6714: Hypoth-

esis on the interaction of Ioxynil with the D1 protein. Z. Naturforsch 45c:436–440, 1990.
55. Draber, W., Hilp, U., Likusa, H., Schindler, M., Trebst, A. Inhibition of photosynthesis by 4-nitro-6-alkylphenols: Structure-activity in wild type and five mutants of *Chlamydomonas reinhardtii* thylakoids. Z. Naturforsch 48c:213–223, 1993.
56. Trebst, A., Hilp, U., Draber, W. Response in the inhibitor efficiency of substituted phenols on PS II activity in six mutants of the D1 protein subunit in *Chlamydomonas reinhardtii*. Phytochemistry 33:969–977, 1993.
57. Jansen, M.A.K., Depka, B., Trebst, A., Edelman, M. Engagement of specific sites in the plastoquinone niche regulates degradation of the D1 protein in photosystem II. J. Biol. Chem. 268:21246–21252, 1993.
58. Oettmeier, W., Masson, K., Höhfeld, J. [^{125}I]Azido-ioxynil labels Val249 of the Photosystem II D-1 reaction center protein. Z. Naturforsch 44c:444–449, 1989.
59. Trebst, A., Draber, W. Inhibitors of photosystem II and the topology of the herbicide and Q_B binding polypeptide in the thylakoid membrane. Photosyn. Res. 10:381–392, 1986.
60. Ajlani, G., Kirilovsky, D., Picaud, M., Astier, C. Molecular analysis of *psbA* mutations responsible for various herbicide resistance phenotypes in *Synechocystis* 6714. Plant Mol. Biol. 13:469–479, 1989.
61. Gingrich, J.C., Buzby, J.S., Stirewalt, W.L., Bryant, D.A. Genetic analysis of two new mutations resulting in herbicide resistance in the cyanobacterium *Synechococcus* sp. PCC 7002. Photosyn. Res. 16:83–99, 1988.
62. Ajlani, G., Meyer, I., Astier, C., Vernotte, C. Inhibition of photosystem II by ioxynil in wild type and resistant mutant of *Synechocystis* 6714. Z. Naturforsch 44c:979–984, 1989.
63. Hawoth, P., Steinback, K.E. Interaction of herbicides and quinone with the Q_B-protein of the diuron-resistant *Chlamydomonas reinhardtii* mutant Dr2. Plant Physiol. 83:1027–1031, 1987.
64. Erickson, J.M., Rahire, M., Rochaix, J.-D., Mets, L. Herbicide resistance and cross-resistance: Changes at three distinct sites in the herbicide-binding protein. Science 228: 204–207, 1985.
65. Pucheu, N., Oettmeier, W., Heisterkamp, U., Masson, K., Wildner, G.F. Metribuzin-resistant mutants of *Chlamydomonas reinhardtii*. Z. Naturforsch 39c:437–439, 1983.
66. Johanningmeier, U., Bodner, U., Wildner, G.F. A new mutation in the gene coding for the herbicide-binding protein in *Chlamydomonas*. FEBS Lett. 211:221–224, 1987.
67. Rochaix, J.-D., Erickson, J. Function and assembly of photosystem II: Genetic and molecular analysis. Trends Biochem. Sci. 13:56–59, 1988.